Supporting Information

Potential apoptosis inducing agents based on a new benzimidazole Schiff base ligand and its dicopper(II) complex

Anup Paul,[a] Rakesh Kumar Gupta,[a] Mrigendra Dubey,[a] Gunjan Sharma,[b] Biplab Koch,[b] Geeta Hundal,[c] Maninderjeet Singh Hundal,[c] and Daya Shankar Pandey*[a]

[a]Departments of Chemistry and [b]Zoology, Faculty of Science, Banaras Hindu University, Varanasi - 221 005 (U.P.) India

[c]Department of Chemistry, Guru Nanak Dev University, Amritsar - 143005 (Punjab), India

---

Table of contents: **Pages**

Experimental Section

Materials and Physical methods

The reagents were procured from commercial sources and used as received without further purification. Solvents were dried and distilled prior to their use following standard procedures.[1] 3-(4,5-dimethylthiazol-2-yl)-2,5-diphenyltetrazolium bromide (MTT), and RPMI-1640 were procured from Hi-Media, ethidium bromide (EB) from Loba Chemie, acridine orange (AO) from Sisco Research Laboratory (SRL) Mumbai, India and calf thymus (CT DNA) from Bangalore Genei, India. 2-(2-aminophenyl)-1-*H*-benzimidazole, salicylaldehyde, iodomethane and sodium hydride were procured from Sigma Aldrich Chemical Co., and used without further purifications.

Elemental analyses for C, H, and N were performed on an Exeter Analytical Inc. model CE-440 CHN analyzer. IR and electronic absorption spectra were acquired on a Varian 3300 FT-IR, and Shimadzu UV-1601, respectively. Fluorescence spectra were recorded on a LS-55 Fluorescence Spectrometer (Perkin-Elmer, UK). The excitation and emission slit widths were set at 10.0 and 3.0 nm, respectively and temperature was maintained by recycling water using peltier system. ^{1}H (300 MHz) and ^{13}C (75.45 MHz) NMR spectra at rt were obtained on a JEOL AL300 FT-NMR spectrometer using tetramethylsilane [$Si(CH_3)_4$] as an internal reference. Electrospray ionization mass spectrometric (ESI-MS) measurements were made on a Bruker Daltonics Amazon SL ion trap mass spectrometer. Samples were dissolved in 100% methanol with 0.1% formic acid and introduced into the ESI source through syringe pump at a flow rate of

100 μL/h. The capillary voltage was 4500 V, and dry gas flow rate 8 L/min at 300 °C. The MS scan was acquired for 2.0 min and spectra print outs were averaged of over each scan.

Synthesis and characterization

Synthesis of 2-(1-methyl-1-*H*-benzo[d]imidazol-2-yl)aniline (A)

To a solution of 2-(2-aminophenyl)-1-*H*-benzimidazole (227 mg, 1 mmol) in dry DMF (5 mL) an ice cooled suspension of sodium hydride (36 mg, 1.5 mmol; 60% dispersion in mineral oil, pre- washed with hexane) in dry DMF (5 mL) was added drop wise over 15 minutes, then cooling bath was removed and the reaction mixture stirred for an additional 24 h. Completion of the reaction was monitored by TLC and after filteration solvent was removed under reduced pressure. Residue thus obtained was partitioned between ethyl acetate and water, after separation the combined organic layers were washed with water, brine solution, and dried on Na_2SO_4. Decantation followed by removal of the solvent under reduced pressure afforded crude product which was further purified by silica gel column chromatography (EtOAc: Hexane; 1:9) to afford the desired product. Yield: 70% . Anal. Calcd. for $C_{14}H_{13}N_3$: C, 75.31; H, 5.87; N, 18.82 Found C, 75.41; H, 5.92; N, 18.72 %. ^{1}H NMR ($CDCl_3$, δ ppm): 3.83 (s, 3H, C$\underline{H}_3$), 5.04 (s, 2H, N$\underline{H}_2$), 7.79 (s, 1H, H-1), 6.76-7.25 (m, 5H, H-3, H-4), 6.80 (d, J = 6.2, 2H, H-2).

Synthesis of 2-(1-methyl-1-*H*-benzimidazol-2-yl)phenyl)imino)methyl)phenol (HL)

It was synthesized by following general procedure described in the literature.[2] To an ethanolic solution (50 mL) of 2-(1-methyl-1-*H*-benzimidazol-2-yl)aniline (224 mg, 1 mmol), salicylaldehyde dissolved in ethanol (5 ml, 122 mg, 1 mmol) and catalytic amounts of acetic acid were added and reaction mixture refluxed for 5 h. After completion of the reaction (monitored by TLC) volume of the reaction mixture was reduced to ~10 mL. Diethyl ether (5 mL) was added to it and solution left undisturbed at -4 ºC. After 4–5 days light yellow needle shaped crystals appeared which were separated by filteration washed with diethylether and dried in air. Yield: 75%. Melting point: 185 °C. Anal. Calcd for $C_{21}H_{17}N_3O$: C, 77.04; H, 5.23; N, 12.84%. Found: C, 76.95; H, 5.31; N, 12.95 %. IR (KBr pellets, cm^{-1}): $\nu_{C=N}$: 1676. ^{1}H NMR ($CDCl_3$, δ ppm): 12.21 (s, 1H, O$\underline{H}$), 8.59 (s, 1H, C(H)=N, H-1), 7.82 (s, 1H, H-2), 7.79 (d, J = 7.2, 2H, H-3), 7.66 (s, 2H, H-4), 7.40-7.29 (m, 5H, H-5), 6.83 (d, J = 8.5, 2H, H-6), 3.68 (s, 3H, -CH_3) . ^{13}C NMR ($CDCl_3$, δ ppm): 164.2; 160.8; 152.0; 147.8; 143.0; 135.7; 133.5; 132.5; 131.9; 131.3; 127.0; 125.5; 122.8; 122.3; 119.8; 119.0; 118.9; 118.9; 109.6, 30.9. ESI-MS (m/z): $[(M + H)]^+$ Calcd

328.1372 , found 328.1535, $[(M + Na)]^+$. Calcd 350.1269, found 350.1354. UV/vis. (**(**H_2O:DMSO; 95:5), λ_{max}, nm, ε M^{-1} cm^{-1}): 280 (1.92×10^4).

Synthesis of [{Cu(L)(NO_3)}$_2$] (CuL)

$CuNO_3 \cdot 3H_2O$ (242 mg, 1 mmol) dissolved in methanol (10 mL) was added drop wise to a methanolic solution (15 mL) of **HL** (327 mg, 1 mmol) and the reaction mixture stirred for 1 h. Resulting solution was filtered and left for slow evaporation. After a few days an olive-green microcrystalline product deposited which was separated by filtration washed with diethylether and dried under vacuuo. Yield: 45%. Anal. Calcd for $C_{42}H_{32}Cu_2N_8O_8$: C, 55.81; H, 3.57; N, 12.40%. Found: C, 55.92; H, 3.42; N, 12.29%. IR (KBr pellets, cm^{-1}): IR ν(C=N): 1617; ν(Cu-ONO_2): 1384. ESI-MS (m/z): $[Cu(L)]^+$ Calcd., 389.0589, found 389.1642. UV/vis. ((**(**H_2O:DMSO, 95:5), λ_{max}, nm, ε M^{-1} cm^{-1}): 289 (3.9×10^4), 396 (5.60×10^3).

X-ray Structure Determinations

Crystals suitable for X-ray single crystal analyses for **HL** and were obtained by slow diffusion of ethanol: diethyl ether and methanol, respectively. X-ray data for these were collected on a Bruker Kappa Apex-II diffractometer at RT with Mo-Kα radiation (λ = 0.71073 Å) at Department of Chemistry, Center for Advanced Studies, Guru Nanak Dev University, Amritsar. Structures were solved by direct methods (SIR-92)[3]and refined by full-matrix least squares on F^2 (SHELX 97).[4] All the non-H atoms were treated anisotropically. H atoms were attached geometrically except for those attached to two water molecules in the structure of **HL**. These were located from difference Fourier synthesis and were refined with Uiso of 1.2 times that of the oxygen atoms and with fixed distances of 0.82(2) Å.

Cell cycle analysis with PI staining

The DNA content during cell cycle steps has been evaluated by flow cytometry. Besides other typical features, apoptotic cells are characterized by DNA fragmentation and consequently, loss of nuclear DNA content. The use of a fluorochrome such as propidium iodide (PI) that is capable of binding and labeling DNA makes it possible to obtain a rapid and precise evaluation of the cellular DNA content by flow cytometric analysis and subsequent identification of the hypodiploid cells.[5] Herein in a experiments 1×10^5 MCF-7 cells were treated with different

concentrations of **HL** and **CuL**. Concentrations of the drug have been chosen on the basis of their IC_{50} values. After 24 h of treatment the cells were trypsinised, washed with 1 mL of phosphate buffered saline (PBS) and fixed in ice cold 70% ethanol and incubated for overnight at -20^{o} C and washed twice with PBS. These were treated with 100 μL of staining solution [960 μL of 0.1% (v/v) Triton x-100, 20 μL of PI (1 mg/mL) and 20 μL of RNase (10 mg/mL, PBS)], and incubated for 30 min at rt in dark. After staining the DNA by PI the samples were evaluated by a flow meter.

DNA Interaction Studies

Electronic absorption titration studies were carried out using a fixed concentration of compounds in DMSO solution (1%) with increasing concentration of CT DNA in 5 mM Tris HCl/50 mM NaCl buffer, pH 7.5 following earlier procedure.[6] Purity of the CT DNA was verified by electronic absorption studies following the ratio of absorbance at 260 and 280 nm, gives 1.9 and suggested that the DNA was sufficiently free of protein. The DNA concentration per nucleotide was determined by examining the molar extinction coefficient of 6600 M^{-1} cm^{-1} at 260 nm. An analogous method was used for emission studies also. Ethidium bromide (EB) displacement experiments were performed by monitoring the changes in fluorescence intensity at excitation and emission wavelengths (λ_{ex}, 525; $\lambda_{em,}$ 602 nm) after aliquot additions of compounds to the Tris-HCl buffer of EB bounded DNA (EB-DNA).

Protein Binding Studies

In protein binding studies the excitation and emission wavelengths of BSA at 280 and ~348 nm were monitored using BSA (1.0 μM) solution prepared in Tris-HCl buffer (pH-7.5) and stored in a dark place at 4 °C. Synchronous fluorescence spectral studies were performed at two different $\Delta\lambda$ values (difference between the excitation and emission wavelengths of BSA), such as 15 and 60 nm, using similar concentration of the BSA and compounds.

Molecular Docking

Molecular docking studies on **HL** and **CuL** have been performed using HEX 6.1 software and Q-site finder which is an interactive molecular graphics program for the interaction, docking calculations, and to identify possible binding site of the biomolecules.[7] Before subjecting the ligand **HL** and complex **CuL** for docking studies, the CIF file of the respective **HL** and **CuL** were saved as a .mol file and were further converted to .pdb format using CHIMERA 1.5.1

software. The crystal structure of B-DNA (PDB ID: 1BNA) and human serum albumin (PDB ID: 1HA2) were obtained from the protein data bank (http://www.rcsb.org./pdb). Visualization of the docked systems has been performed using Discovery Studio 3.5 software. The by default parameters used for docking calculation with correlation type shape only, FFT mode at 3D level, grid dimension was 6 with receptor range 180 and ligand range 180 with twist range 360 and distance range 40.

Cell Viability and Proliferation Assay/MTT Assays

Cell viability was checked by MTT assay which is a colorimetric assay based on the conversion of the yellow tetrazolium salt MTT to purple formazan crystals after reacted with mitochondrial dehydrogenase of metabolically active cells.[8] Stock solutions of ligand (**HL)** as well as complex (**CuL)** was prepared in DMSO and diluted with DMEM (The final concentration of DMSO did not exceeded 0.5% v/v). MCF-7 cells (2×10^4 cells per well) were plated in 96-well culture plates and 5 replica wells were used for controls as well as treated groups. After 24 h, culture medium was replaced by fresh medium containing various concentrations of **HL** and **CuL** and incubated for 24 h in a 5% CO_2 humidified atmosphere. After 24 h of drug exposure, medium was removed and 100 μL medium and 10 μL of 5 mg/mL MTT in phosphate buffered saline (PBS, pH 7.4) was added to each well for an additional 2 h. Then the medium and MTT were removed and 100 μL of DMSO was added to dissolve the MTT formazan crystals. The absorbance of samples was measured at 570 nm with ELISA plate reader. Cytotoxicity effect was revealed as the percentage of treated cells relative to untreated cells at A570 nm. Percent control was calculated using the following formula:

% Control = [Mean O. D. of Drug treated well / Mean O. D. of control well] × 100

Cell cycle analysis with PI staining and Morphological Analysis by AO/EB Staining

The DNA content during cell cycle steps was evaluated with flow cytometry. Beside other typical features apoptotic cells are characterized by DNA fragmentation and consequently, loss of nuclear DNA content. Use of a fluorochrome, such as PI (propidium iodide), that is capable of binding and labeling DNA makes it possible to obtain a rapid and precise evaluation of cellular DNA content by flow cytometric analysis, and subsequent identification of hypodiploid cells.[9] For the experiment, 2×10^5 MCF-7 cells were treated with different concentrations of **HL** and

CuL. Concentration of drugs was chosen based on their IC_{50} values. After 24 h of treatment the cells were trypsinised and washed in 1 mL of PBS (phosphate buffered saline) and cells were fixed in ice cold 70% ethanol and incubated for overnight at -20^{o} C. Then the cells were washed twice in PBS. Next 100 μL of staining solution [960 μL of 0.1% (v/v) Triton x-100 solution, 20 μL of PI (1 mg/mL) solution and 20 μL of RNase (10 mg/mL in PBS)] was added in each sample and incubated for 30 min at room temperature in the dark. After staining of DNA by PI, samples were evaluated by a flow cytometer.

To study the apoptosis in cells, morphological analysis were done using fluorescent dyes acridine orange and ethidium bromide (AO/EB). AO is a cell membrane permeable cationic dyes, entered into the cells and stained DNA with green color appearance, and allow the visualization of the chromatin pattern. Staining with AO, the viable cells appear green with green nucleus whereas early apoptotic cells with condensed or fragmented nuclei. However EB can enter only in non-viable cells thereby the nucleus appears bright orange overwhelming the AO stain.[10] Briefly, 2×10^5 cells were seeded on cover slip in 6 well plates with DMEM containing 10% FBS and treated with 11, 22 and 33 μM of **CuL** and 305, 458 and 610 μM of **HL** respectively for 24h. Cells were washed with PBS and stained with 50 μL of EB solution and 50 μL of AO solution having stock of 100 μg/mL each in PBS. The stained cells were washed twice with PBS and cover slips were put on glass slide and photographs were taken by Nikon 800 fluorescence microscope at 40X.

This technique is used to distinguish viable cells, early apoptotic cells with blebbing and necrotic cells. AO intercalates into the DNA and gives a green fluorescence and thus, the viable cells appear with a green nucleus while early apoptotic cells with condensed or fragmented nuclei. EB is taken up only by the nonviable cells giving a bright orange nucleus of the dead cells, overwhelming the AO stain.[10]

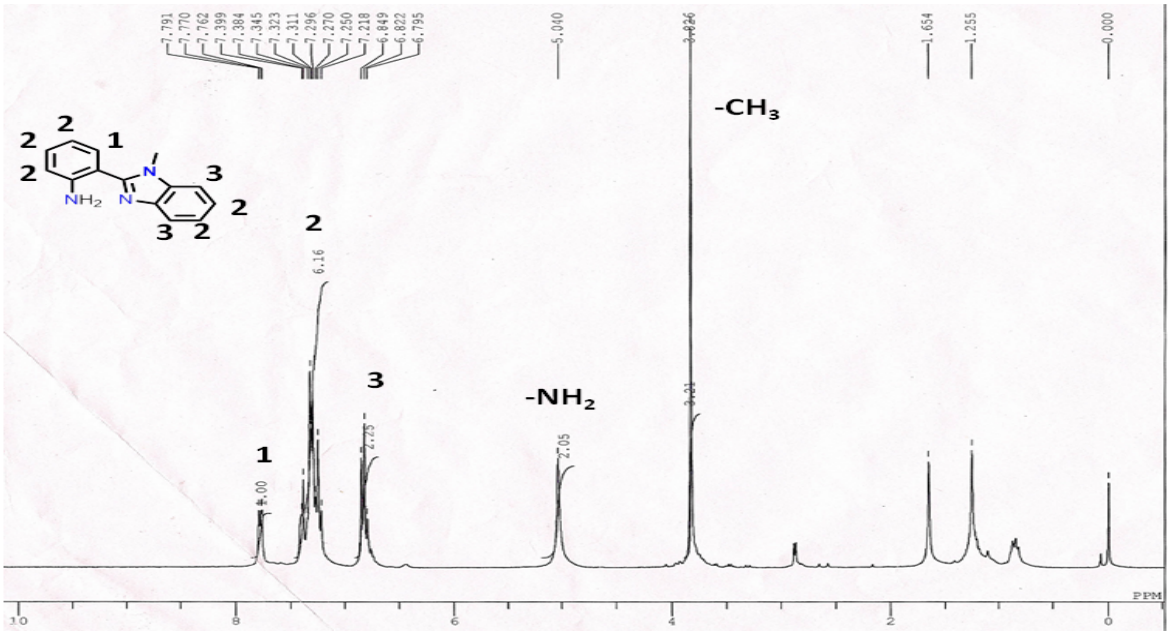

Figure A. 1H-NMR Spectrum of **A**

Figure S1. Infrared spectrum og **HL** and **CuL**.

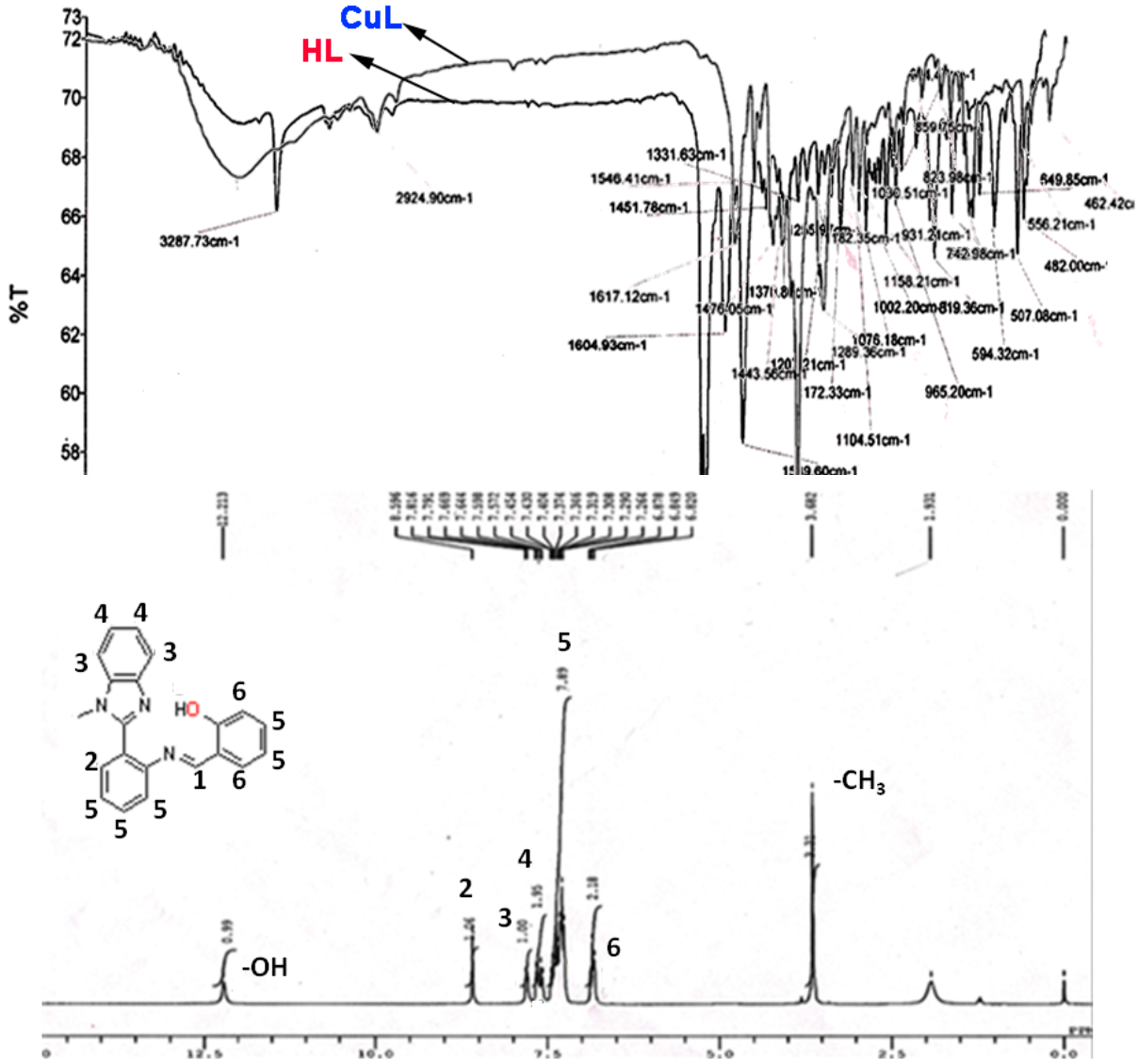

Figure S2. ^{1}H-NMR Spectrum of **HL**

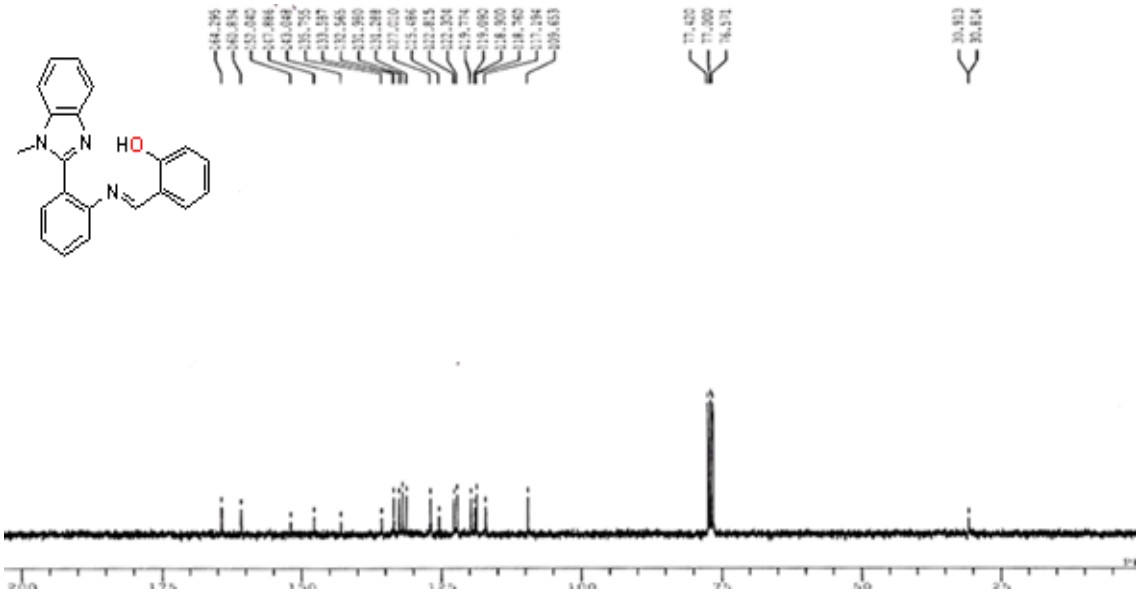

Figure S3. ^{13}C-NMR Spectrum of **HL.**

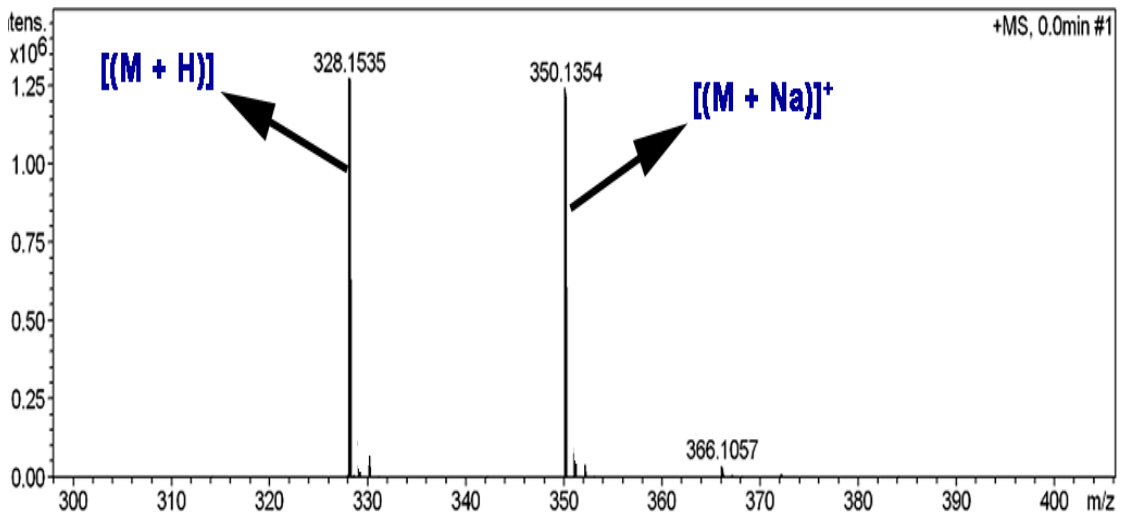

Figure S4. ESI-MS Spectrum of **HL**.

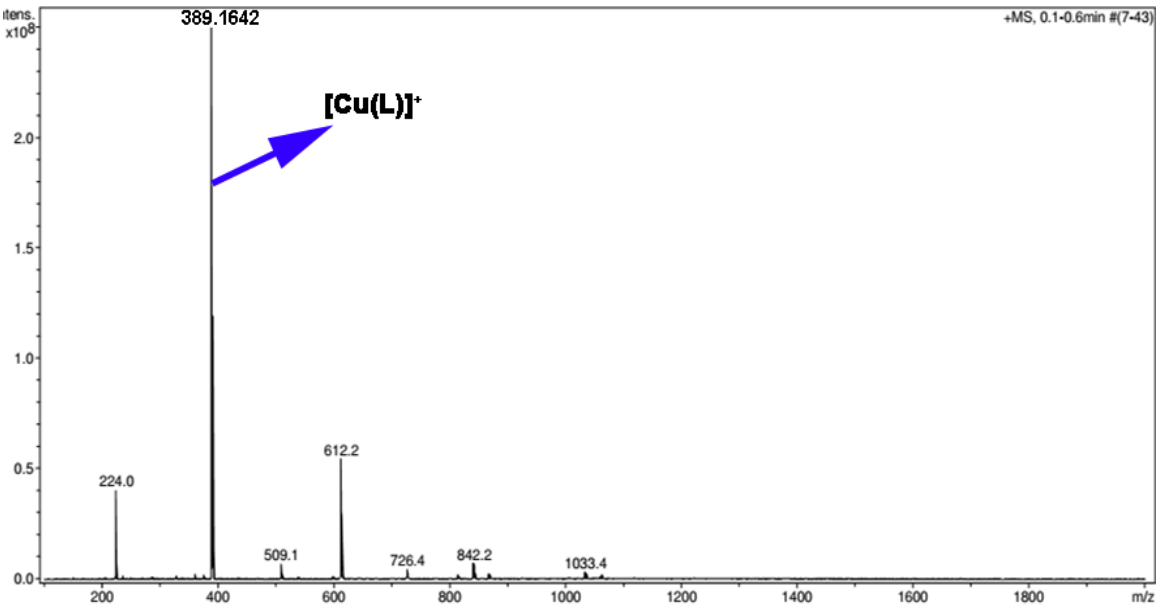

Figure S5. ESI-MS Spectrum of **CuL**.

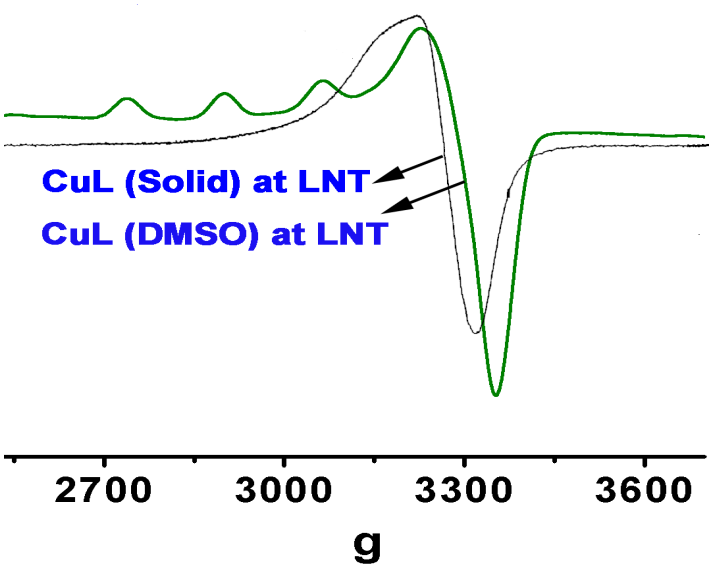

Figure 6. EPR Spectrum of **CuL** in solid and solution (DMSO) at 77K.

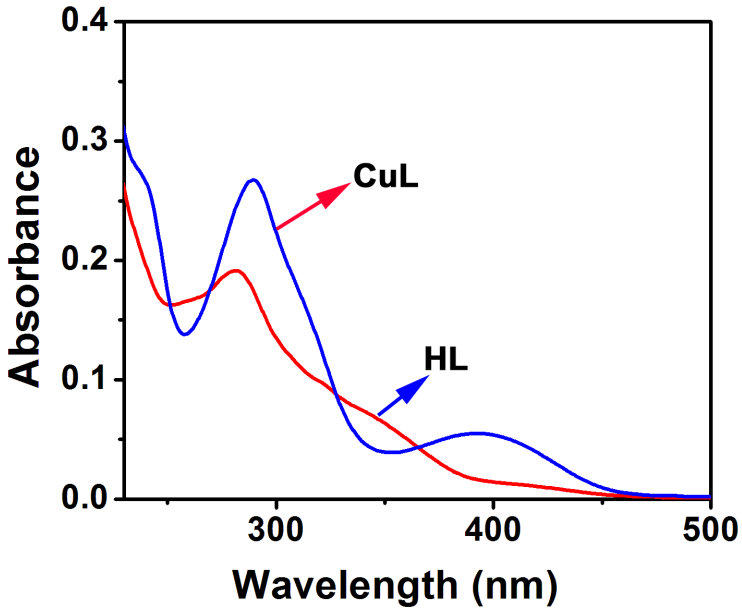

Figure S7. UV/vis spectrum of **HL** and **CuL**.

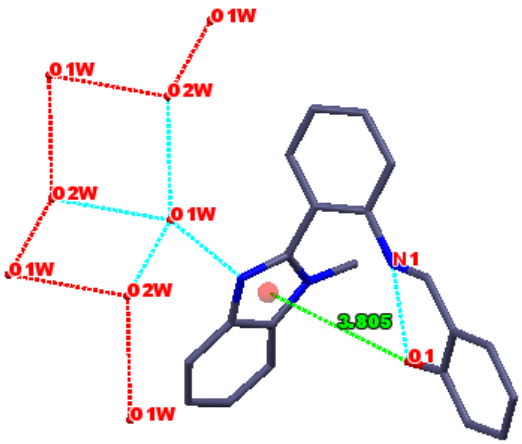

Figure S8. Showing conformation, O-H… π and H-bonding interactions.

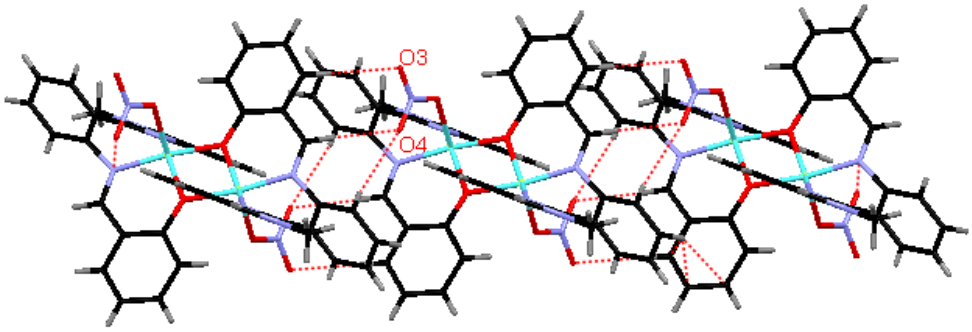

Figure S9. Showing the formation of H-bonded 1D chain due to weak H-bonding with the nitrate groups.

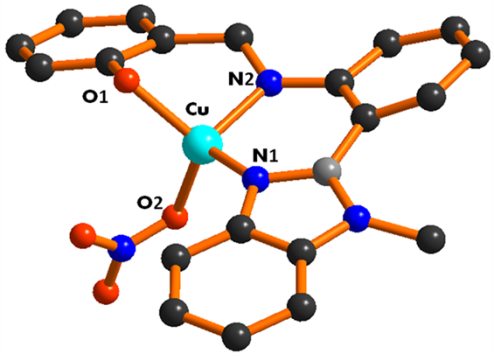

Figure S10. Energy minimized structure of **CuL**. Color code; Cu = cyan, O = red, N = blue, C = grey.

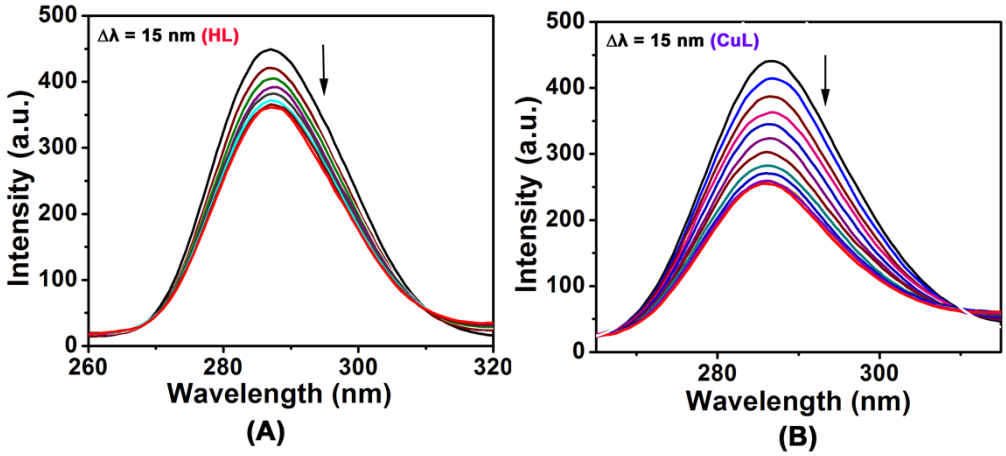

Figure S11. Synchronous spectrum of BSA (1×10^{-6} M) in the presence of increasing amount of **HL**(A) and **CuL** (B) (0–30 μM) in the wavelength difference of $\Delta\lambda$ = 15. Arrow shows the emission intensity changes upon increasing concentrations.

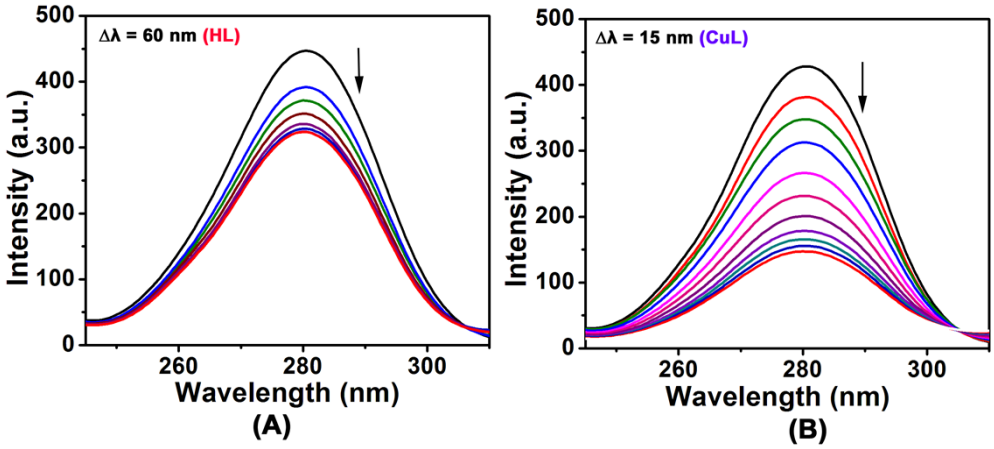

Figure S12. Synchronous spectrum of BSA (1×10^{-6} M) in the presence of increasing amount of **HL**(A) and **CuL** (B) (0–30 μM) in the wavelength difference of $\Delta\lambda$ = 60. Arrow shows the emission intensity changes upon increasing concentrations.

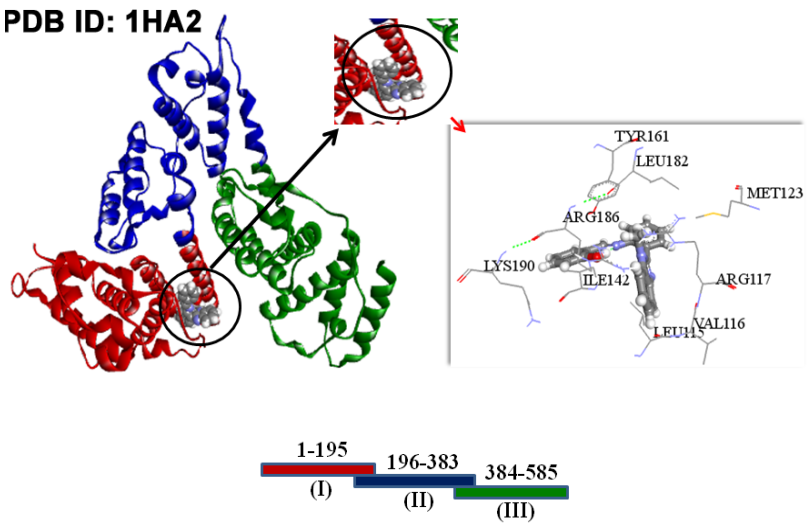

Figure S13. Molecular docked model of **HL** with HSA (PDB ID: 1HA2).

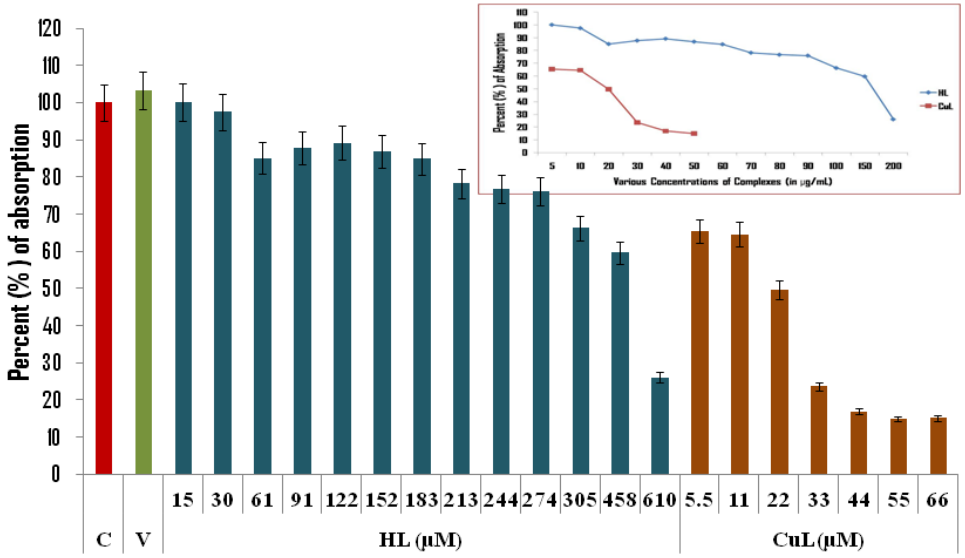

Figure S14. Cell viability of MCF-7 breast cancer cells after drug treatment for 24 h by MTT assay: effect of **HL** and **CuL** on cell survival. Inset shows comparison between **HL** and **CuL**.

Table S1. Selected bond lengths (Å) and angles (°) for **HL** and **CuL**

HL			
Bond length (Å)		**Bond Angle (°)**	
C8-C13	1.401(3)	C7-N1-C8	121.2(2)
C8-N1	1.412(3)	C1-C6-C7	121.1(2)
C7-C5	1.275(3)	O1-C1-C6	121.5(2)
C6-C1	1.393(4)	N2 -C14- C13	122.6(2)
C1-O1	1.341(3)	C14 -N2- C21	127.4(2)
C13-C14	1.475(3)		
C14-N2	1.363(3)		
C21-N2	1.452(3)		
CuL			
Bond length (Å)		**Bond Angle (°)**	
N3-Cu1	1.946(3)	N2-C7-C9	123.2(3)
N4-O1	1.269(4)	C1-N2-Cu1	129.7(2)
N4-O2	1.232(4)	C14-N3-Cu1	115.8(2)
N4-O3	1.229(4)	C15-N3-Cu1	124.7(3)
Cu1-O1	2.245(3)	N4-O1-Cu1	125.9(2)
Cu1-O4	1.975(2)	C17-O4-Cu1	126.2(2)
Cu1-O4^{1}	1.966(2)	C17-O4-Cu1^{1}	130.1(2)
Cu1^{1}-O4	1.966(2)	Cu1^{1}-O4-Cu1	101.61(10)
Cu1^{1}-O4^{1}	1.975(2)	N2-Cu1-O1	110.07(12)
Cu1-Cu1^{1}	3.0550(10)	N3-Cu1-O1	91.30(11)
		N3-Cu1-O4^{1}	171.42(11)
		O4^{1}-Cu1-N2	99.03(11)
		O4-Cu1-O1	109.20(11)
		O4^{1}-Cu1-O1	90.33(10)
		O4^{1}-Cu1-O4	78.39(10)

Table S2 Showing important H-bonding interactions in HL (Å,°)

	Donor...Acceptor	H...Acceptor	Donor-H.....Acceptor
O1-H1...N1	2.581(3)	1.85	147
O1-H1...N2	3.349(3)	2.78	128
O1W-H11W...N3	2.894(3)	2.04(2)	167
O1W-H12W...O2Wi	2.996(4)	2.15(2)	170
O2W-H21W...O1Wii	2.876(3)	1.99(2)	172
O2W-H22W...O1Wiii	3.040(4)	2.18(3)	170

(i) -x+1,-y+1,-z+1, (ii) x,+y-1,+z, (iii) -x,-y+1,-z+1

References

1 D. D. Perrin, W. L. F. Armarego and D. R. Perrin, Purification of Laboratory Chemicals; Pergamon Press: Oxford, 1980.

2 G. Zakrzewski and L. Sacconi, *Inorg. Chem*., 1968, **7**, 1034.

3 A. Altomare, G. Cascarano, C. Giacovazzo and A. Guagliardi, *J. Appl. Crystallogr.*, 1994, **27**, 435.

4 G. M. Sheldrick, *Acta Crystallogr., Sect. A*: 2008, **A64**, 112.

5 (a) T. Bezabeh, M. R. A. Mowat, L. Jarolim, A. H. Greenberg and I .C. P. Smith, *Cell death and Differentiation,* 2001, **8**, 219. (b) C, Riccardi and I. Nicoletti, *Nat Protoc*., 2006, **1**, 1458.

6 (a) R. K. Gupta, G. Sharma, R. Pandey, A. Kumar, B. Koch, P. Li, Q. Xu, and D. S. Pandey, *Inorg. Chem.*, 2013, **52**, 13984. (b) R. K. Gupta, R. Pandey, G. Sharma, R. Prasad, B. Koch,

S. Srikrishna, P. Li, Q. Xu, and D. S. Pandey, *Inorg. Chem.*, 2013, **52**, 3687

7 D. Mustard and D. W. Ritchie, *Proteins: Struct. Funct. Bioinf.,* 2005, **60**, 269.

8 T. J. Mosmann, *Journal of Immunological Methods,* 1983, **65**, 55.

9 T. Bezabeh, M. R. A. Mowat, L. Jarolim, A. H. Greenberg and I .C. P. Smith, *Cell Death and Differentiation.* 2001, 8, 219. (b) C, Riccardi and I. Nicoletti, *Nat Protoc*., 2006, 1(3), 1458.

10 A. J. McGahon, S. J. Martin, R. P. Bissonnette, A. Mahboubi, Y. Shi, R. J. Mogil, W. K. Nishioka and D. R. Green, *Methods Cell Biol.,* 1995, **46**, 153.